Bending Motions and Internal Motions in Myosin Rod[†]

Stefan Highsmith,* Chun-Chen Wang, Karl Zero, R. Pecora, and Oleg Jardetzky

ABSTRACT: Depolarized light scattering and high-resolution ^{1}H NMR measurements were made on solutions of light meromyosin (LMM) and myosin rod in 0.6 M KCl–0.010 M pyrophosphate, pH 9.5, at 20 °C. The light scattering data indicated LMM is a rigid molecule. Myosin rod is best described as a once-broken rod with domains that can freely diffuse in conical volumes. The maximum angle that the cone surface makes with the myosin rod axis is 128°, indicating the bending motion of the domains is largely unrestrained. NMR data indicated the fraction of the structure that could be in a random-coil configuration was equal and less than 0.04 for both hydrodynamically rigid LMM and bending myosin rod. Thus, the flexible bending of myosin rod appears to not be due to a random-coil structure.

Ohe of the mechanical requirements of myosin in the contemporary models of chemomechanical energy transduction is that it be flexible in the 144-nm-long cylindrical rod portion of the molecule. This flexibility would allow myosin rod to bend near its center, so that the ATPase portions of myosin could move away from the thick filament toward the actin thin filament (Huxley, 1969). The ATPase portions (called subfragment 1's or S-1's) move distances that vary as much as 4 nm during contraction (Elliot et al., 1965), so myosin rod bending or stretching must provide an adjustable mechanical linkage between S1 and the thick filament. About 80 nm of myosin rod has a structure that is insoluble under physiological conditions. This portion [called light meromyosin (LMM)][1] causes myosin to aggregate into thick filaments. The remaining portion of myosin rod (called subfragment 2 or S-2) connects LMM and the S-1's and should be attached to LMM by a flexible mechanical linkage. Figure 1 shows the mechanical features of myosin rod that are required. The bendable region is referred to as a "hinge". In addition to flexibility, it has been suggested that elasticity is a property of the S-2 portion of myosin in muscle. This could provide a restoring force for stretching (Huxley & Simmons, 1971) and/or bending (Highsmith, 1981) motions that occur in tension generation, or perhaps provide the tension itself (Harrington, 1971).

Many experiments on myosin have suggested or been compatible with a bendable myosin rod. These experiments have been reviewed in detail (Harvey & Cheung, 1981). Two reports of direct measurements of myosin rod flexibility have been made. Electrical birefringence measurements on solutions of LMM, S-2, and myosin rod at pH 9.3 indicated that LMM was rigid and that S-2 and myosin rod were flexible (Highsmith et al., 1977). Fluorescence depolarization measurements on fluorescently labeled myosin rod were interpreted to show that it was flexible at pH 4 (Harvey & Cheung, 1977). Both methods demonstrated flexibility as a rate of rotational Brownian motion too fast for a linear rigid cylinder the dimensions of myosin rod. No signal from the segmental bending motion of the constituent LMM or S-2 portions was detected in either case. At pH ≥6, the fluorescence depolarization measurements suggested that myosin rod did not bend freely. A model of myosin rod that can bend but not freely is consistent with viscoelastic measurements on myosin (Rosser et al., 1978); however, the pH dependency of the chemical cross-linking of S-2 to the thick filament core suggests that hinge flexibility is enhanced at high pH (Sutoh et al., 1978), not reduced, in agreement with the electric birefringence measurements at high pH.

The molecular structure responsible for the flexibility of the hinge region of myosin is not known. Myosin rod is composed of two α helixes in a coiled-coil configuration. The rapid selective proteolysis of myosin in the hinge region has been interpreted to indicate that the region has some random-coil structure that is especially susceptible to hydrolysis and that allows bending to occur. This possibility, although often mentioned, has little experimental support. The amino acid content of the region is high in glycine (Lu, 1980), an amino acid associated with non-α-helical structure (Fasman et al., 1976); however, optical rotatory dispersion and circular dichroism measurements indicate that myosin rod is greater than 95% α helix (Cohen & Szent-Gyorgi, 1957).

In the study reported here, the hydrodynamic rotational motion and the bending motion of myosin rod and LMM in solution at high pH containing pyrophosphate were investigated by dynamic depolarized light scattering measurements, and the fraction of their structures that could be random coil was determined by high-resolution ^{1}H NMR spectroscopy. It was confirmed that LMM is rigid and myosin rod is flexible at high pH. In addition, a signal from a rapidly moving domain compatible with S-2 and LMM was detected for myosin rod and shown to be freely bending in the volume of a slightly restricted cone. The amount of structure that could be in a random-coil structure was limited to about 3.6% for both myosin rod and LMM. Thus, the hydrodynamically flexible myosin rod and the rigid LMM have the same amount of structure that is internally mobile. Finally, support for a theory on the properties of semidilute rigid cylindrical molecules was obtained from the light scattering measurements on LMM.

Experimental Procedures

Proteins and Chemicals. Myosin was prepared from New

* Correspondence should be addressed to this author at the Department of Biochemistry, School of Dentistry, University of the Pacific.

[1] Abbreviations: S-1, myosin subfragment 1; S-2, myosin subfragment 2; LMM, light meromyosin; ^{1}H NMR, proton nuclear magnetic resonance; τ, rotational correlation time.
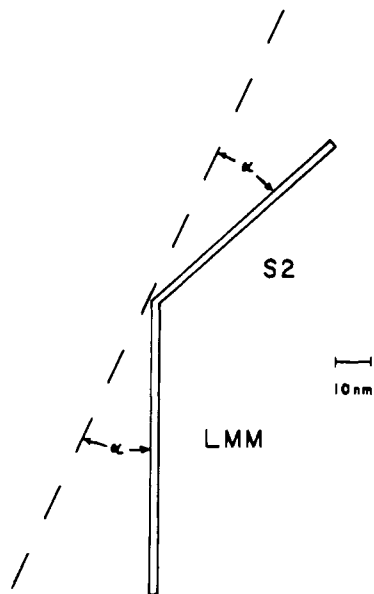
FIGURE 1: Structure of myosin rod. Myosin rod is composed of two domains connected by a flexible region called a hinge. The LMM portion and the S-2 portion are 79 and 65 nm long, respectively. The bending motion of myosin rod is characterized by the angle α that defines the conical volumes through which the domains are free to diffuse.

Zealand rabbit doral muscle by the method of Nauss et al. (1969); LMM was prepared from myosin by the method of Lowey et al. (1969); myosin rod was prepared from myosin by the method of Balint et al. (1975) as modified by Goodno et al. (1976). LMM and myosin rod had negligible Ca^{2+}–ATPase activity as determined by the pH-stat method. As reported earlier, polyacrylamide gel electrophoresis of LMM and myosin rod in the presence of sodium dodecyl sulfate produced single bands corresponding to the appropriate molecular weights (Highsmith et al., 1977). Protein solutions were dialyzed to the appropriate conditions and centrifuged at 80000g for 1 h before measurements were made. Samples for light scattering were filtered through Nucleopore filters (0.22-μm pores) to remove dust particles. Concentrations of LMM and myosin rod were estimated from the absorbance of 280-nm light by using $\epsilon^{1\%}_{280nm}$ = 2.00 (Brahms & Brezner, 1961) and molecular weights of 1.4×10^5 and 2.5×10^5, respectively.[2] All measurements were made within 4 days after the fragments were prepared. Between measurements, samples were kept at 5 °C.

Light Scattering Measurements. Light from the 488-nm line of an argon ion laser (Spectra Physics Model 165) was passed through a polarizer and focusing lens onto the sample cells. The scattered light at 90° passed through an analyzer, pinhole, lens, pinhole sequence and was detected with an EMI 9502-RF photomultiplier tube with an SSR amplifier discriminator (Model 1120). A Malvern 48 channel clipped correlator was used to find the time autocorrelation functions of the scattered light intensity. The data were then transferred to a Data General Nova 3 computer, stored on floppy disks, and analyzed.

---

[2] A referee pointed out to us that Margossian & Lowey (1978) have determined $\epsilon^{1\%}_{280nm}$ to be larger for LMM than for myosin rod. If so, none of the conclusions in this study regarding myosin rod flexibility would be changed. The range of the linear portion of Figure 5 would be reduced, and β' would be smaller. However, these are not crucial in any way, and we have used the same value of $\epsilon^{1\%}_{280nm}$ for LMM and myosin rod so that the results in this paper are directly comparable to those from earlier electrical birefringence measurements (Highsmith et al., 1977).
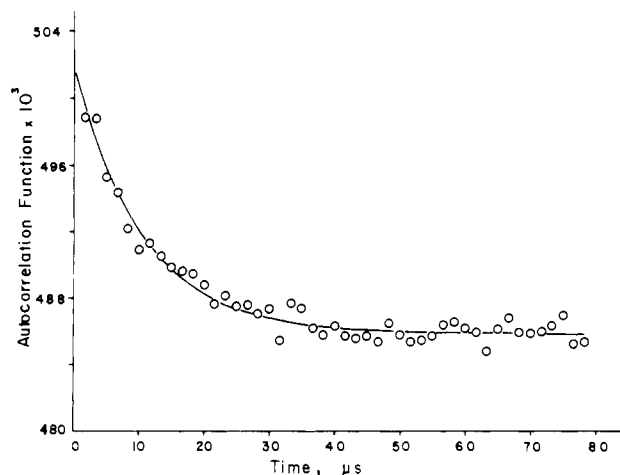

FIGURE 2: Typical light scattering data. Autocorrelation function of the intensity of the depolarized scattered light for a 6 mg/mL solution of myosin rod in 0.6 M KCl–0.010 M pyrophosphate, pH 9.5, at 20 °C. Points were obtained at 2-μs intervals. The solid line is a fit of eq 3 to the data.

The correlation functions were fit by nonlinear least-squares analysis to the following equations:

$$C(t) = A + B \exp(-2t/\tau) \qquad (1)$$

$$C(t) = A + B_1 \exp(-2t/\tau_1) + B_2 \exp(-2t/\tau_2) \qquad (2)$$

$$C(t) = A + [B_{1'} \exp(-t/\tau_{1'}) + B_{2'} \exp(-t/\tau_{2'})]^2 \qquad (3)$$

where A, B, B_1, B_2, $B_{1'}$, and $B_{2'}$ are constants for a given scattering vector length q and incident light intensity, τ_1, τ_2, $\tau_{1'}$, $\tau_{2'}$, and τ are time constants, and t is time. More details are given in Zero & Pecora (1982a). Typical laser power was about 1 W for the depolarized data and a few tenths of a watt for the polarized data. The polarized data were collected on a 10 μs/channel time scale, and the depolarized data were collected on 1 μs/channel and 2 μs/channel time scales. Due to after-pulsing from the phototube, the first 4 μs was ignored for the depolarized data. All data were collected at a regulated temperature of 20.0 °C.

^1H *NMR Measurements.* Protein solutions were dialyzed to the appropriate buffers in ^2H_2O before measurements. All spectra were obtained by using a modified Bruker HXS-360 spectrometer and quadrature detection. The sweep width was typically ±3000 Hz. A 75° pulse and a 1- or 2-s delay time was used. The temperature was maintained to ±0.5 °C. The ^2H_2O signal was not suppressed because this has been shown to reduce the broad peaks in the myosin spectrum (Akasaka et al., 1978). Chemical shifts are given in parts per million from external tetramethylsilane.

The fraction of a total spectrum that appears in the narrow peaks, corresponding to the fraction of the structure displaying internal mobility, was determined by methods described elsewhere (Highsmith et al., 1979). In brief, the narrow peak fraction is determined by resolution enhancement, which eliminates the broad components of the spectrum (Gassner et al., 1978), or by cutting and weighing. The two methods give the same result. The crucial requirement in this approach is that the spectrum includes all of the broad component. LMM and myosin rod have larger rotational correlation coefficients than the proteins analyzed earlier by this method, so some of the broad peaks might be too broad to detect. The total area was determined for differing sweep widths near 3000 Hz to avoid this artifact. It was unchanged by these changes in preacquisition delay time. A second method of ensuring that none of the broad component was lost to compare the
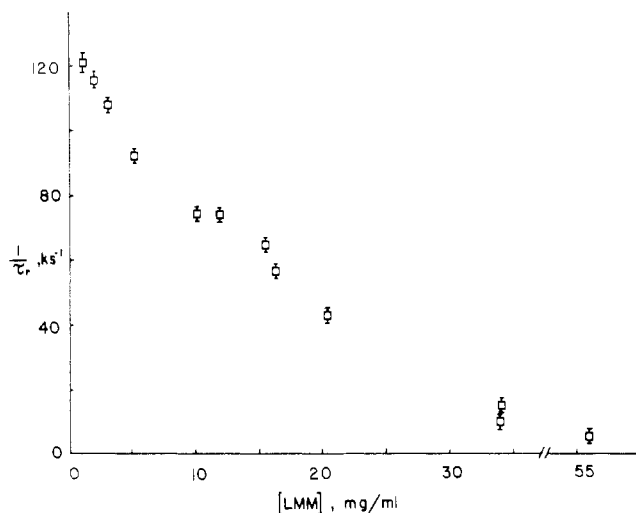
FIGURE 3: Rotational correlation times for LMM. Values for $1/\tau_r$ obtained by using eq 1 are plotted as a function of [LMM].

native protein spectral area (minus the buffer area) to the base-denatured protein spectral area (minus the denaturing buffer area). The latter presumably has no broad components. When this was done, all spectra were obtained with no changes in any instrumental or computational settings.

Results

Depolarized Light Scattering. A typical autocorrelation function for the depolarized light scattered from a solution of myosin rod is shown in Figure 2. Curves of this type were obtained for solutions of LMM and myosin rod over a range of concentrations and analyzed by fitting eq 1–3 to the data points as described under Experimental Procedures and in Zero & Pecora (1982a).

The results obtained for solutions of LMM in 0.6 M KCl–10 mM pyrophosphate, pH 9.5, at 20 °C when fit by eq 1 are shown in Figure 3. The decrease in the apparent rate of rotational Brownian motion as the concentration increases will be discussed below. The extrapolated value of $1/\tau_r$ for very dilute solutions is 130 ks^{-1}. The relaxation data were well fit by a single exponential at all concentrations and were not better fit by two exponentials. The extrapolated value for $1/\tau_r$ obtained by electrical birefringence for LMM, corrected to the same temperature and viscosity, was 131 ks^{-1} (Highsmith et al., 1977). If LMM were a rigid cylinder of length 79.1 nm, it would have $1/\tau_r = 140$ ks^{-1} (Broersma, 1960). The theoretical value is slightly larger than the experimental values, but is in good agreement. τ_r is proportional to the cube of the length of the molecule so the difference might be due to a small underestimation of the length of LMM used to obtain the theoretical value. The results indicate that LMM is a rigid linear molecule.

The results for myosin rod are shown in Figure 4. The middle points show $1/\tau_r$ fit by eq 1 as a function of concentration. The concentration range is lower than that of LMM, and there is little concentration dependence. The average is $1/\tau_r = 46 \pm 5$ ks^{-1}. As shown in Table I, this value is too large for a rigid cylinder as predicted by Broersma (1960) and is in reasonable agreement with the value obtained from electrical birefringence measurements on similar solutions. The data for myosin rod were better fit as a sum of two exponentials squared (eq 3) than as one exponential (Figure 1, the uppermost and lowest sets of points). The slower time constant, 23 ± 6 ks^{-1}, is closer to the value for a rigid rod and probably reflects the overall rotational motion of the molecule. Much
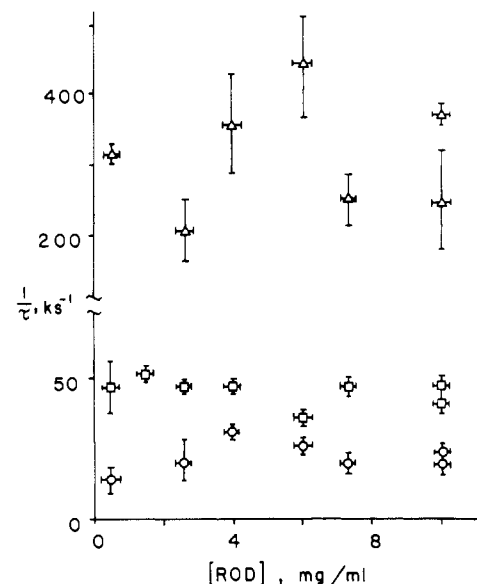

FIGURE 4: Rotational correlation times for myosin rod. Values for $1/\tau$ are plotted as a function of [myosin rod]. The squares are for a single exponential fit (eq 1). The circles and triangles are for a two-exponential fit (eq 3).

Table I: Rotational Brownian Motion and Bending Motion of Myosin Rod and LMM (τ_r^{-1} in ks^{-1} at 20 °C)

protein	from depolarized light scattering measurements	from electrical birefringence measurements[a]	calcd for a rigid cylinder[b]
LMM	130 ± 5[c]	131 ± 2	140
myosin rod	46 ± 5[c] or 315 ± 80 and 23 ± 6[d]	41.5 ± 1	32.2

[a] Highsmith et al. (1977) corrected to 20 °C. [b] Broersma (1960), using the contour length and a diameter of 2 nm. [c] Equation 1, subtracting $q^2D = 5$ ks^{-1}. [d] Equation 3, subtracting $q^2D = 5$ ks^{-1}.

better agreement with the value predicted for a rigid cylinder is obtained if the data for $t > 8$ μs are fit to a single exponential, thus eliminating most of the fast component. In that case, the slow time component is 29 ± 5 ks^{-1}.

A recent theory developed to analyze the light scattering spectrum of an angularly restricted once-broken rod was used to obtain the maximum angle of bending (assuming free diffusion in a cone) and the time constant for the bending motion (Zero & Pecora, 1982a). Applying this theory, we estimated the maximum angle of bending to be 128° (error range 121–132°), indicating the rotation is somewhat restricted. Unrestricted rotation would correspond to a value of 180°. The fast time constant in the theory is

$$1/\tau_{fast} = \nu(\nu + 1)D_\beta + 6\theta + q^2D$$

where D_β is the diffusion coefficient for the bending motion, θ is the diffusion coefficient for overall rotation, q is the length of the scattering vector, D is the translational diffusion coefficient, and ν has a value near 3 for an angle of 128°. Using a value for D from polarized light scattering measurements on myosin rod and fitting the depolarized light scattering data to eq 4, one obtains $D_\beta = 24 \pm 6$ krad/s for myosin rod. This is only slightly larger than the rotational diffusion coefficient for free LMM, $\theta = 22 \pm 1$ krad/s, obtained by using eq 1 to get $1/\tau_r$ and the expression $1/\tau_r = 6\theta + q^2D$. Thus, a segment of myosin rod is bending with a diffusion coefficient compatible with the rate of rotation of the free segment.
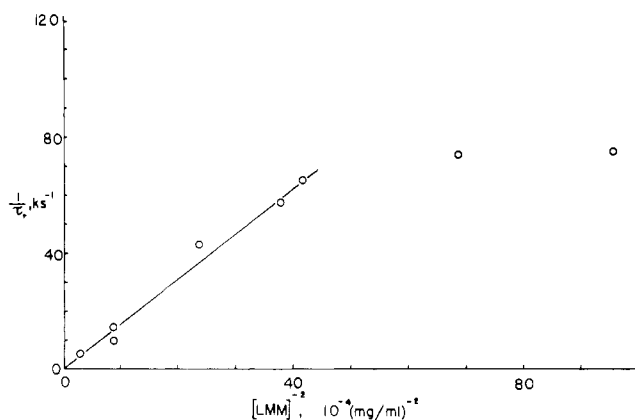
FIGURE 5: Semidilute solutions of rigid cylinders. The data from Figure 4 are replotted according to the theory of Doi & Edwards (1978). The dependence of $1/\tau_r$ on $[LMM]^{-2}$ in the appropriate concentration range is as predicted for a molecule the dimensions of LMM.

The concentration dependence of LMM in Figure 3 could be due to aggregation at higher concentrations. However, the solvent conditions were chosen to minimize aggregation (Harrington & Himmelfarb, 1972). Another explanation is steric repulsion. A theory describing the behavior of rigid cylindrical molecules in solution has been derived by Doi & Edwards (1978) and supported by Zero & Pecora (1982b). This theory assumes the concentration is high enough to show significant intermolecular steric hindrance ($c \gg 1/L^3$, where c is the number concentration and L is the length of a molecule) but still low enough to allow a random distribution [$c < 2\pi/(dL^2)$, where d is the diameter of each molecule]. The equation they obtain for the rotational diffusion coefficient is

$$\Theta = \beta' kT \ln (L/d)/(\eta_s L^9 c^2)$$

where η_s is the solvent viscosity, k is Boltzmann's constant, T is the absolute temperature, and β' is a proportionality constant. When the data from Figure 3 are replotted (Figure 5), the expected linear dependence on the inverse squared concentration is observed for concentrations above ~10 mg/mL. The value found for β' is 390. This indicates it is steric repulsion rather than aggregation that accounts for the concentration dependence in this study and probably in an earlier study on similar solutions (Highsmith et al., 1977). The data for myosin rod are for concentrations too low to show significant steric repulsion.

1H NMR. Spectra (360 MHz) of LMM and myosin rod are shown in Figure 6. The dominant feature in each case is the large broad peak in the aliphatic region (4 to -2 ppm). Some narrow peaks appear at 0.9, 1.3, 1.7, 3.0, 6.7, 7.2, and 7.6 ppm downfield from external tetramethylsilane. The narrow peaks have line widths of less than 50 Hz, and those with shifts greater than 2 are too far downfield to be methyl groups. Peaks this narrow from proteins this size appear to result from localized internal motions of amino acid backbone and side chains (Highsmith & Jardetzky, 1981). Each of the narrow peaks is due to many protons, and no attempt has been made to assign them to specific amino acid side chains.

Two analyses of the NMR data were made. First, the fraction of the total structure which contributes to the spectrum was determined by comparing the area of the native spectra to those of NaO^2H-denatured proteins. Second, the fraction of the structure of the native protein that contributes to the narrow peaks was determined. Both of these analyses have been described (Highsmith et al., 1979) and are discussed for
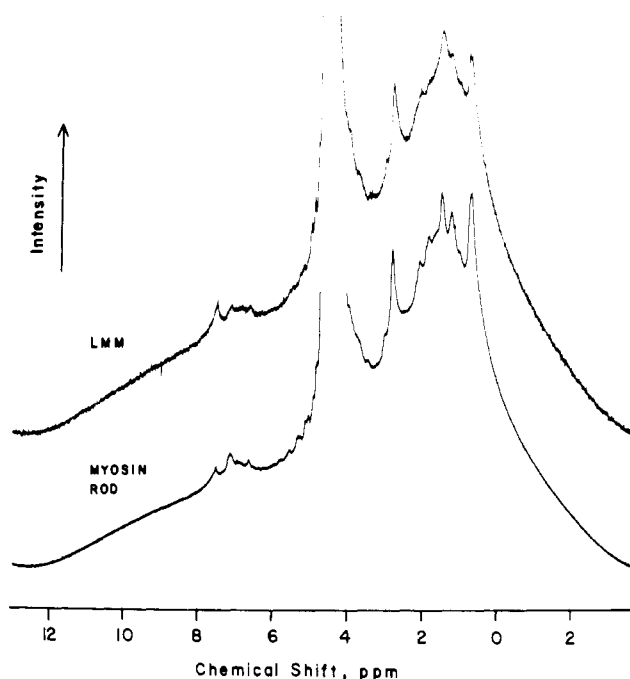

FIGURE 6: *1H* NMR spectra of LMM and myosin rod. Spectra (360 MHz) of 8 mg/mL LMM and 10 mg/mL myosin rod under conditions described in Figure 3. Intensity of the resonance absorption is plotted against the chemical shift from external tetramethylsilane in ppm.

Table II: Fractions of Myosin Rod and LMM *1H* NMR Spectra That Are in Narrow Peaks

protein	concn (mg/mL)	native area/ denatured area	% area in narrow peaks
LMM	3	1.12	3.9
	9	0.91	4.0
	30	0.88	3.0
			3.7 ± 0.8
myosin rod	5	0.82	4.6
	18	1.19	3.3
	27	0.98	2.5
			3.5 ± 0.7

the present case under Experimental Procedures. The results for various concentrations of LMM and myosin rod are shown in Table II. The column "native area/denatured area" is the ratio of the native spectral area to the denatured spectral area, corrected for the contribution from the solvent HO^2H peak. Within the experimental error of about 20%, the results indicate that all of the protein is contributing to native spectra at all the concentrations measured. The average for all the data is 98%. The constancy with concentration supports the conclusion, drawn from the analyses of the concentration dependence of the depolarized light scattering data, that the proteins are not aggregating. Aggregation would produce complexes that are very large and very likely have peaks too broad to be detected.

Since all of the structure of myosin rod and LMM appears to be contributing to their native *1H* NMR spectra, the fraction of the narrow peak area is the fraction of the total structure which displays internal mobility. The "% area in narrow peaks" column in Table II shows these results. Both LMM and myosin rod have about 3.6% of their structures moving rapidly enough to give narrow resonance peaks.

Discussion

The depolarized light scattering data indicate that LMM behaves hydrodynamically as a rigid molecule. The data were

fit adequately as a single exponential decay (eq 1), and the fit was not significantly improved by using two exponential functions. The time constant obtained from the autocorrelation function was in good agreement with the value predicted by Broersma (1960) for a rigid molecule of LMM's dimensions and equal within experimental error to a value obtained by the independent method of electrical birefringence. Thus, there is consistent strong evidence that LMM is hydrodynamically rigid under the conditions used in these experiments. This makes results for LMM useful for comparison to results for the myosin rod. An interesting aside is that the apparent decrease in $1/\tau_r$ with LMM concentration (Figure 3) is probably not due to aggregation but is due to steric repulsion between LMM molecules as they become crowded in solution.

The depolarized light scattering data for myosin rod indicate that it is not rigid with regard to hydrodynamic mobility. A forced single exponential fit to eq 1 gives a time constant that is too short for a rigid molecule of the dimensions of myosin rod. The value for $1/\tau_r$ is in reasonable agreement with that obtained from a single exponential fit to electric birefringence decay data (Highsmith et al., 1977). The enhanced rate of rotation indicates myosin rod is flexible.

A better fit to the myosin rod light scattering data was obtained by using a two-exponential function (eq 3). The error associated with the fitting of a curve is usually reduced by using more variables. However, for myosin rod, the decay time obtained with a single exponential fit was sensitive to the sampling interval used in computing the correlation function. A two-exponential fit, on the other hand, gave consistent fits when the sampling interval was varied. The slow decay time constant from the two-exponential fit approached the predicted value for a rigid myosin rod, and the slow decay time constant obtained by analyzing only the tail of the decay curve gave a value of $1/\tau_r$ that was within 10% of the predicted value. This very likely corresponds to rotation of the entire molecule, which is coupled to other modes of motion sufficiently weakly to be resolved. The fast time constant obtained from the two-exponential fit corresponds to the segmental motion of a domain of myosin rod. This confirms that myosin rod is not flexing its entire length but that it has a hinge, as has been predicted (Huxley, 1969). When the fast time constant was analyzed for bending motions, the bending diffusion coefficient obtained was in good agreement with the rotational diffusion coefficient of LMM. Thus, the rate of bending of a portion of myosin rod is consistent with the motion of its constituents, LMM and S-2. The resolution of the overall and bending motions of myosin rod gives semiquantitative support for the model predicted in the early formulation of the cross-bridge hypothesis of muscular forces generation (Huxley, 1969; Huxley & Simmons, 1971) and is in agreement with recent electron micrographs indicating the rod bends near its center (Takahashi, 1978).

An additional result obtained from the two-exponential fit is the angle of the cone that determines the volume in which the bending segment of myosin rod is free to diffuse. Analysis of the weighting factors in eq 3 (Zero & Pecora, 1982a) indicates the cone includes the volume up to $2\alpha = 128°$ from the axis of the rod (see Figure 1). Takahashi (1978) obtained a value of 145° by an independent method. This is not a large restriction of the bending motion but is quite distinct from no restriction. It is reasonable to attribute the restriction to steric hindrance of bending due to the fact that the molecule is not a line but a coiled coil of α helixes that occupy space themselves or to charge–charge repulsion as LMM and S-2 get close. These results are not compatible with a myosin rod that

has a substantial intrinsic restoring force opposing the bending motions.

The proton NMR results indicate that the structure responsible for the flexibility of myosin rod is not a random coil or some other conformation lacking secondary structure. The fraction of myosin that could be assigned to a random-coil structure is less than 0.04. This is an upper limit, since the areas of broad rather than narrow resonance peaks are likely to be underestimated due to artifacts. The simplest argument against flexibility being due to a random-coil structure comes from the fact that LMM, which is rigid, has the same fraction of structure that could be assigned to such a conformation as the flexible myosin rod. The notion that flexibility is due to a secondary structure free hinge region of myosin came from its trypsin susceptibility. Since molecules as small as N-acetylarginamide are good substrates for trypsin, not much of the structure of myosin rod need be free of secondary structure. It seems more likely that the hinge region of myosin is different from the rest of myosin rod in ways that are subtle and that the flexible region that allows bending has significant secondary structure.

References

Akasaka, K., Konrad, M., & Goody, R. (1978) FEBS Lett. 96, 287–290.

Balint, M., Streter, F. A., & Gergely, J. (1975) Arch. Biochem. Biophys. 168, 557–566.

Brahms, J., & Brezner, J. (1961) Arch. Biochem. Biophys. 95, 219–228.

Broersma, S. (1960) J. Chem. Phys. 32, 1626–1631.

Cohen, C., & Szent-Gyorgi, A. G. (1957) J. Am. Chem. Soc. 79, 248.

Doi, M., & Edwards, S. F. (1978) J. Chem. Soc., Faraday Trans. 2 74, 918–929.

Elliott, G., Lowy, J., & Millman, R. (1965) Nature (London) 206, 1357–1358.

Fasman, G., Chou, P. Y., & Adler, A. J. (1976) Biophys. J. 16, 1201–1238.

Gassner, M., Jardetzky, O., & Conover, W. W. (1978) J. Magn. Reson. 30, 141–146.

Goodno, C. C., Harris, T. A., & Swenson, C. A. (1976) Biochemistry 15, 5157–5160.

Harrington, W. F. (1971) Proc. Natl. Acad. Sci. U.S.A. 68, 685–689.

Harrington, W. F., & Himmelfarb, S. (1972) Biochemistry 16, 2945–2952.

Harvey, S., & Cheung, H. (1977) Biochemistry 16, 5181–5187.

Harvey, S., & Cheung, H. (1981) in Muscle and Non-Muscle Motility (Dowben, R., & Shay, J., Eds.) Chapter 5, Plenum Press, New York.

Highsmith, S. (1981) Biochim. Biophys. Acta 639, 31–39.

Highsmith, S., & Jardetzky, O. (1981) Biochemistry 20, 780–783.

Highsmith, S., Kretzschmar, K. M., O'Konski, C. T., & Morales, M. F. (1977) Proc. Natl. Acad. Sci. U.S.A. 74, 4986–4990.

Highsmith, S., Akasaka, K., Konrad, M., Goody, R., Holmes, K., Wade-Jardetzky, N., & Jardetzky, O. (1979) Biochemistry 18, 4238–4244.

Huxley, H. E. (1969) Science (Washington, D.C.) 164, 1356–1366.

Huxley, A. F., & Simmons, R. (1971) Nature (London) 233, 533–538.

Lowey, S., Slater, H. S., Weeds, A. G., & Baker, H. (1969) J. Mol. Biol. 42, 1–29.

Lu, R. C. (1980) *Proc. Natl. Acad. Sci. U.S.A. 77,* 2010–2013.

Margossian, S. S., & Lowey, S. (1978) *Biochemistry 17,* 5431–5439.

Nauss, K. M., Kitagawa, S., & Gergely, J. (1969) *J. Biol. Chem. 244,* 755–765.

Rosser, R. W., Nestler, F. H. M., Shrag, J. L., Ferry, J. D., & Greaser, M. (1978) *Macromolecules 11,* 1239–1242.

Sutoh, K., Chiao, Y.-C. C., & Harrington, W. F. (1978) *Biochemistry 17,* 1234–1239.

Takahashi, K. (1978) *J. Biochem. (Tokyo) 83,* 905–908.

Zero, K., & Pecora, R. (1982a) *Macromolecules* (in press).

Zero, K., & Pecora, R. (1982b) *Macromolecules 15,* 87–93.

Photoinduced Calcium Release from Rhodopsin–Phospholipid Membrane Vesicles[†]

Patricia N. Tyminski, Richard T. Klingbiel, Rebecca A. Ott, and David F. O'Brien*

ABSTRACT: Brief blue-green light exposure of rhodopsin–phospholipid membrane vesicles that contained divalent cations released the cations from the vesicles. The photoinduced release is due to an increase in permeability of the membrane. The quantity of ions released depends on the initial ionic concentration inside the vesicles. At 37 °C and an internal concentration of 30 mM Ca^{2+}, the initial flux for rhodopsin–egg phosphatidylcholine membrane vesicles was 0.25 ± 0.11 Ca^{2+} per bleached rhodopsin per s. Similar fluxes were observed for the release of Co^{2+}, Mn^{2+}, Ni^{2+}, and Mg^{2+}. The addition of proton uncouplers and lipophilic anions accelerated the rate to ~1 Ca^{2+} per bleached rhodopsin per s. The flux was independent of the concentration of rhodopsin in the membranes and sensitive to the head-group composition of the rhodopsin–phospholipid vesicles. Analysis of the fraction of Ca^{2+} released and the fraction of bleached rhodopsin per vesicle showed that a single bleached rhodopsin per vesicle is necessary and sufficient for Ca^{2+} release. Ca^{2+} release was not observed from thermally bleached rhodopsin. These results are discussed with regard to the possible role of Ca^{2+} as an excitatory transmitter in vision.

Light absorption by the 11-*cis*-retinal chromophore of rhodopsin isomerizes the chromophore and initiates visual excitation (Wald, 1968). Excitation of the rod cell causes a hyperpolarization of its potential (Tomita, 1965; Bortoff & Norton, 1965), because of a reduction of the rod outer segment (ROS)[1] plasma membrane permeability (Hagins, 1972; Korenbrot & Cone, 1972). It is generally accepted that a transmitter is necessary to mediate between the light-activated rhodopsin in the disk membranes of the ROS and the site of the sodium permeability in the plasma membrane (Baylor & Fuortes, 1970).

Hagins (1972) proposed that the transmitter is calcium ion that is released from the disks into the ROS cytoplasm on light exposure of rhodopsin. In electrophysiological experiments, the addition of calcium to a retina mimicked the effect of light (Yoshikami & Hagins, 1973; Hagins & Yoshikami, 1974; Brown et al., 1977; Lipton et al., 1977), and the addition of EGTA to a retina attenuated the effect of light (Hagins & Yoshikami, 1977; Brown et al., 1977). Osmotic measurements on isolated ROS's demonstrated that the addition of calcium to the buffer reduces the sodium permeability of the plasma membrane (Bownds & Brodie, 1975; Wormington & Cone, 1978) and depresses the cyclic GMP levels in the ROS (Woodruff & Bownds, 1979). It has been demonstrated that calcium is present in sufficient quantities inside the disk membranes to serve as the transmitter (Liebman, 1974; Szuts & Cone, 1977). Although these data support the hypothesis that calcium is the transmitter in ROS membranes, clear evidence for the photorelease of calcium from disk membranes in sufficient quantities and with the proper time course has yet to be achieved. It has been estimated that $10–10^3$ transmitter molecules per bleached rhodopsin need to be released in ~10^{-1} s (Cone, 1973; Yoshikami & Hagins, 1973).

Several attempts to measure the photoinduced release of calcium from various ROS disk preparations have been reported. Many were summarized by Smith et al. (1977), who reported that the photorelease of $^{45}Ca^{2+}$ from sonicated ROS disks occurred with a yield of 0.75 Ca^{2+} per bleached rhodopsin at high levels of bleaching (24–100%). Smith & Bauer (1979) found somewhat larger releases at lower bleach levels (~2 Ca^{2+} per bleached rhodopsin at 5% bleaching), but the release required ~10^2 s. Szuts & Cone (1977) evaluated the photorelease of endogenous calcium from freshly isolated dark-adapted frog ROS disks by atomic absorption analysis and did not observe a significant release within a few seconds at low bleach levels (0.01% bleaching).

Photoinduced permeability change of rhodopsin–phospholipid membrane vesicles has also been reported (O'Brien et al., 1977b; Hubbell et al., 1977; Darszon et al., 1977; O'Brien, 1979; Gold & Korenbrot, 1979). Light exposure of rhodopsin–phospholipid membrane vesicles, which are closed unilamellar bilayers, increases the permeability of the vesicles to divalent cations without destroying the bilayer (O'Brien, 1979).

---

[1] Abbreviations: ROS, rod outer segment; EGTA, ethylene glycol bis(β-aminoethyl ether)-*N,N,N',N'*-tetraacetic acid; cyclic GMP, guanosine cyclic 3',5'-phosphate; Hepes, *N*-(2-hydroxyethyl)piperazine-*N'*-2-ethanesulfonic acid; Pipes, piperazine-*N,N'*-bis(2-ethanesulfonic acid); PC, phosphatidylcholine; PE, phosphatidylethanolamine; PS, phosphatidylserine; DOPC, dioleoylphosphatidylcholine; CCCP, carbonyl cyanide *m*-chlorophenylhydrazone; meta I, metarhodopsin I; meta II, metarhodopsin II; Rh, rhodopsin; BRh, bleached rhodopsin; ND, neutral density; GTPase, guanosinetriphosphatase.